

Cold filaments in galaxy clusters: effects of heat conduction

Carlo Nipoti^{*} and James Binney^{*}

Theoretical Physics, Oxford University, 1 Keble Road, Oxford OX1 3NP, UK

Resubmitted 2004 January 8

ABSTRACT

We determine the critical size l_{crit} of a filament of cold ($T \sim 10^4$ K) gas that is in radiative equilibrium with X-ray emitting gas at temperatures $T_{\text{out}} \sim 10^6 - 10^8$ K. Filaments smaller than l_{crit} will be rapidly evaporated, while longer ones will induce the condensation of the ambient medium. At fixed pressure P , l_{crit} increases as $T_{\text{out}}^{11/4}$, while at fixed T_{out} it scales as P^{-1} . It scales as $f^{1/2}$, where f is the factor by which the magnetic field depresses the thermal conductivity below Spitzer’s benchmark value. For plausible values of f , l_{crit} is similar to the lengths of observed filaments. In a cluster such as Perseus, the value of l_{crit} increases by over an order of magnitude between the centre and a radius of 100 kpc. If the spectrum of seed filament lengths l is strongly falling with l , as is natural, then these results explain why filaments are only seen within a few kiloparsecs of the centres of clusters, and are not seen in clusters that have no cooling flow. We calculate the differential emission measure as a function of temperature for the interface between filaments and ambient gas of various temperatures. We discuss the implications of our results for the origin of the galaxy luminosity function.

Key words: conduction – cooling flows – galaxies: clusters: general – galaxies: formation

1 INTRODUCTION

Intergalactic space within clusters of galaxies contains enormous quantities of gas that is at the virial temperature. In about three quarters of all rich clusters, the temperature falls by a factor of 2 to 3 within a few tens of kiloparsecs of the cluster centre – such clusters are said to possess a ‘cooling flow’. Nearby examples are the Virgo, Hydra and Perseus clusters.

Optical emission-line filaments are observed around NGC 1275 at the centre of the Perseus cluster (Minkowski 1957; Lynds 1970; Conselice, Gallagher & Wyse 2001, and reference therein). Similar structures of extended H α emission are seen near the centres of other cooling-flow clusters (e.g., Virgo, Hydra, A2597, A2052, A1795; see Heckman 1981; Hu, Cowie & Wang 1985; Johnstone, Fabian & Nulsen 1987; Heckman et al. 1989). The origin of these filaments and the mechanism responsible for their ionization have been extensively studied, but definitive conclusions have not been reached. Two formation scenarios have been proposed. In the first, the filaments

form as the intracluster medium (ICM) cools (e.g., Fabian & Nulsen 1977, Cowie, Fabian & Nulsen 1980). In the other scenario, filaments are produced through cosmic infall of either cold gas or gas-rich galaxies (e.g., Soker, Bregman & Sarazin 1991; Baum 1992; Sparks 1992). The fact that filaments are observed *only* in clusters with cooling flows has often been considered evidence for the first scenario, but by no means all cooling-flow clusters have detectable optical emission lines (e.g., A2029; see Fabian 1994). Some observational data favour the infall scenario. For example, Sparks, Macchetto & Golombek (1989) showed that filaments contain dust with normal Galactic extinction properties, which filaments formed by condensation of the ICM should not (see also Donahue & Voit 1993). In addition, the filaments appear to be dynamically disturbed systems, suggesting that they form through violent processes, such as merging, rather than through the quiescent condensation of the X-ray emitting ICM.

An important related question is, what mechanism is responsible for heating the filaments? Many possible ionization sources have been considered: Active Galactic Nuclei (AGN); shocks; massive stars; radiation from the ICM; magnetic reconnection (e.g., Heckman et al.

^{*} E-mail: nipoti@thphys.ox.ac.uk (CN); binney@thphys.ox.ac.uk (JB)

1989). None of these ionization mechanisms, individually, can satisfactorily account for the observed emission-line ratios and intensities, so possible combinations of these processes have been explored (e.g., Sabra, Shields & Filippenko 2000). However, there are indications that the heating source is physically associated with the filaments (Conselice et. al 2001 and references therein). Thus, it is likely that stellar photoionization makes an important contribution to powering their optical emission-lines, since young stars are systematically found in the filaments (e.g., McNamara, O'Connell & Sarazin 1996).

The existence of cool filaments embedded in hot ambient plasma has implications for the problem of the plasma's thermal conductivity, which must be moderated by the intracluster magnetic field. If the conductivity were high, one would expect the filaments to evaporate rapidly. Thus, in principle, their very existence limits the conductivity in the same way that of cold fronts in the ICM does (Markevitch et al. 2000, 2003). Given our very limited understanding of the connectedness of the intergalactic magnetic field, and the possibility that thermal conductivity contributes significantly to the global dynamics of cooling flows (Narayan & Medvedev 2001, Voigt & Fabian 2003 and references therein), observational constraints on thermal conductivity are valuable.

In this paper we address two main questions:

- (i) Why are cold filaments observed only in cooling-flow clusters? and why only in the cluster core?
- (ii) To what degree does the existence of these filaments constrain the thermal conductivity of the ICM?

The competition between evaporation and condensation when a cool body of plasma is immersed in a hotter ambient medium has been studied extensively in the literature (Graham & Langer 1973; Cowie & McKee 1977; McKee & Cowie 1977; Balbus & McKee 1982; Giuliani 1984; Draine & Giuliani 1984; Balbus 1986; Böhringer & Hartquist 1987; Böhringer & Fabian 1989; McKee & Begelman 1990; Ferrara & Shchekinov 1993). Most effort has been devoted either to spherical clouds or to planar inhomogeneities, although Cowie & Songaila (1977) considered spheroidal clouds. Since the morphology of observed filaments suggests that cylindrical symmetry should provide a useful idealization, we revisit the problem for this case, and discuss the implications of our results for real systems.

In any geometry, clouds below some critical size are evaporated, while clouds above this size grow by condensation of the hot medium. We determine the critical size that separates these two regimes by finding the steady-state solution in which conductivity exactly balances radiative losses. The typical size of observed filaments is likely to be comparable to the critical size: much smaller filaments are rapidly evaporated away, while filaments above this critical value grow slowly, at a rate determined by the cooling time. Significantly larger filaments are expected to be very rare: in principle, if they formed they could fundamentally change the nature of the system by eliminating the cooling hot ambient plasma.

In Section 2 we derive the critical cylindrical solution. In Section 3 we discuss the application of the model to cluster filaments. Our conclusions are in Section 4.

2 RADIATIVELY STABILIZED CYLINDRICAL CLOUDS

2.1 Model and equations

We consider a long cylindrically symmetric cloud in which there is perfect balance between conductive heat flow towards the symmetry axis and radiative losses, so the plasma flows neither inwards nor outwards (see McKee & Cowie 1977). The temperature on the axis is assumed to be $T \sim 10^4$ K, while far from the origin T asymptotes to a value $\sim 10^6 - 10^8$ K. With these assumptions, and neglecting the effects of gravity, the energy equation reads

$$-\nabla \cdot \mathbf{q} = n_e^2 \Lambda(T), \quad (1)$$

where \mathbf{q} is the heat flux, n_e is the electron number density, and $\Lambda(T)$ is the normalized cooling function. In the unsaturated thermal conduction regime¹, the heat flux is given by

$$\mathbf{q} = -\kappa(T) \nabla T, \quad (2)$$

with $\kappa(T)$ thermal conductivity. For a hydrogen plasma, in the absence of magnetic fields, Spitzer (1962) derives $\kappa(T) = \kappa_0 T^{5/2}$, with $\kappa_0 \simeq 1.84 \times 10^{-5} (\ln \Lambda)^{-1} \text{ erg s}^{-1} \text{ cm}^{-1} \text{ K}^{-7/2}$, where $\ln \Lambda$ is the Coulomb logarithm, which is only weakly dependent on n_e and T (in the following we assume $\ln \Lambda = 30$). Confinement of thermal electrons by the intracluster magnetic field reduces the actual conductivity to

$$\kappa(T) = f \kappa_0 T^{5/2}, \quad (3)$$

where the parameter $f \leq 1$ is the heat conduction suppression factor (e.g., Binney & Cowie 1981, Böhringer & Fabian 1989).

At least in some clusters, observations indicate that emission-line nebulae are in pressure equilibrium with the surrounding hot plasma (e.g., Heckman et al. 1989). So we require that the pressure $P = n_e T$ is constant throughout the interface, and we use this relation to eliminate n_e in the right-hand side of equation (1). Thus, under the assumption of cylindrical symmetry, eliminating \mathbf{q} with the help of equations (2) and (3), the energy equation (1) is reduced to the differential equation

$$\frac{f \kappa_0}{R} \frac{d}{dR} \left(R T^{5/2} \frac{dT}{dR} \right) = P^2 \frac{\Lambda(T)}{T^2}, \quad (4)$$

where R is the cylindrical radius.

2.2 Boundary conditions

Equation (4) applies outside the edge at R_{in} of the $T \sim 10^4$ K cloud: we assume that the cloud contains its own heat sources, such as photoionizing stars, so on its surface the temperature gradient and heat flux vanish. We require T to attain some specified value on $R = R_{\text{out}}$. Thus we solve equation (4) subject to three boundary conditions, $T(R_{\text{in}}) = T_{\text{in}} = 10^4$ K, $dT/dR(R_{\text{in}}) = 0$, and $T(R_{\text{out}}) = T_{\text{out}}$, the temperature of the ambient

¹ In the Appendix we discuss the possible effects of saturation.

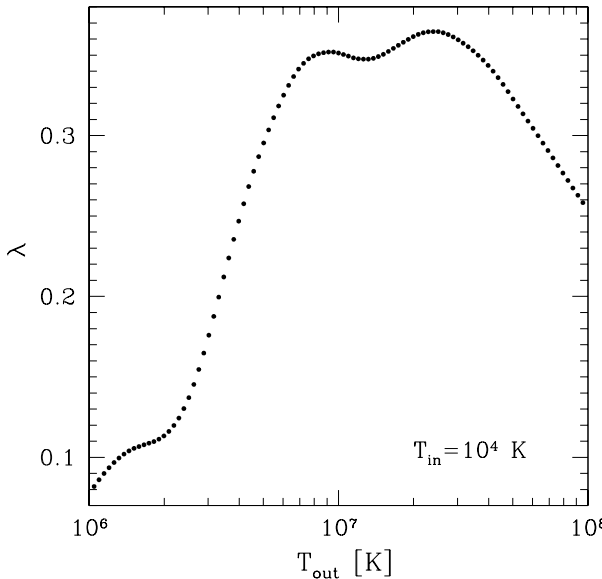


Figure 1. Eigenvalues λ of equation (5) for a set of values of the outer temperature T_{out} .

hot plasma, which varies with distance from the cluster centre. For completeness we will explore the wide range $10^6 \lesssim T_{\text{out}} \lesssim 10^8$ K.

Introducing the dimensionless quantities $\xi = R/R_{\text{out}}$, $\tau = T/T_{\text{out}}$, and $\tilde{\Lambda}_{T_{\text{out}}}(\tau) \equiv \Lambda(\tau T_{\text{out}})/\Lambda_{23}$, with $\Lambda_{23} = 10^{-23} \text{ erg s}^{-1} \text{ cm}^3$, equation (4) reads

$$\frac{1}{\xi} \frac{d}{d\xi} \left(\xi \tau^{5/2} \frac{d\tau}{d\xi} \right) = \lambda \frac{\tilde{\Lambda}_{T_{\text{out}}}(\tau)}{\tau^2}, \quad (5)$$

where

$$\lambda = \frac{P^2 R_{\text{out}}^2 \Lambda_{23}}{f \kappa_0 T_{\text{out}}^{11/2}} \quad (6)$$

is an unknown dimensionless parameter that is the eigenvalue of equation (5). Expressed in dimensionless variables, the boundary conditions are $\tau(\xi_{\text{in}}) = \tau_{\text{in}}$, $d\tau/d\xi(\xi_{\text{in}}) = 0$, and $\tau(1) = 1$ with $\xi_{\text{in}} \equiv R_{\text{in}}/R_{\text{out}}$ and $\tau_{\text{in}} \equiv T_{\text{in}}/T_{\text{out}}$. Due to the presence of $\tilde{\Lambda}_{T_{\text{out}}}$, the eigenfunctions $\tau(\xi)$ and eigenvalues λ depend on the outer temperature T_{out} in addition to the dimensionless numbers ξ_{in} and τ_{in} .

The inner and outer radii R_{in} and R_{out} cannot be exactly identified with observational quantities. However, we can assume that R_{in} corresponds approximately to the width of the filament, and R_{out} to its length l . The latter assumption is consistent with the hypothesis of cylindrical geometry, which does not hold at $R \gtrsim l$. Observed filaments are highly elongated, with ratios length/width $\gtrsim 100$ (Conselice et al. 2001). Thus, we explore a range of values of ξ_{in} that satisfy $\xi_{\text{in}} \ll 1$.

2.3 Numerical solutions

Equation (5) is non-linear and would require numerical integration even if $\tilde{\Lambda}_{T_{\text{out}}}(\tau)$ were approximated by a simple analytical function. Thus, use of the tabulated cooling

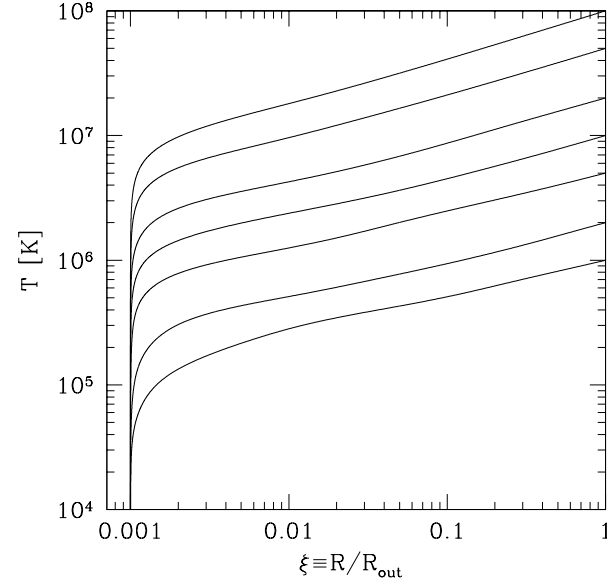


Figure 2. Temperature profile $T(R)$ corresponding to the eigenfunction $\tau(\xi)$ of equation (5), for $T_{\text{out}} = 0.1, 0.2, 0.5, 1, 2, 5, 10$, in units of 10^7 K.

function of Sutherland & Dopita (1993) for metallicity $[\text{Fe}/\text{H}] = -0.5$ introduces no additional computational complexity. We use a shooting method, with Newton iteration, to calculate the solutions.

Numerical integration of equation (5) shows that, for any fixed T_{out} in the range considered, the value of λ is virtually independent of ξ_{in} , provided that ξ_{in} is sufficiently small (i.e., $\xi_{\text{in}} \lesssim 10^{-2}$). Thus, in what follows we can simplify our treatment by assuming that the eigenvalue λ depends only on T_{out} .

Although the details of the *inner* temperature profile $\tau(\xi)$ depend significantly on ξ_{in} , the behaviour of the profile at $\xi \gtrsim 10^{-2}$ is virtually independent of ξ_{in} provided $\xi_{\text{in}} \lesssim 10^{-3}$. Henceforth we set $\xi_{\text{in}} \lesssim 10^{-3}$ so that *both* λ *and the observationally significant part of* $\tau(\xi)$ *are independent on the exact radial range considered*.

Fig. 1 shows λ as a function of T_{out} , while Fig. 2 shows a number of the corresponding eigenfunctions $T(R)$. For values of T_{out} in the relevant range, λ spans a relatively small range ($0.08 \lesssim \lambda \lesssim 0.37$), which is reduced to $0.25 \lesssim \lambda \lesssim 0.37$ for $T_{\text{out}} \gtrsim 4 \times 10^6$ K.

From Fig. 2 is apparent that over a significant fraction of the radial range the temperature profiles are roughly power laws, with similar indices. This suggests that an approximate analytical solution could be obtained by exploring the asymptotic behaviour of the eigenfunctions of equation (5) for $\xi \rightarrow 1$ ($\tau \rightarrow 1$). When we assume $\tau = \xi^n$, and approximate the cooling function near T_{out} by $\tilde{\Lambda}_{T_{\text{out}}}(\tau) \simeq [\Lambda(T_{\text{out}})/\Lambda_{23}]\tau^\alpha$, equation (5) requires $n = 4/(11-2\alpha)$, and $\lambda = \frac{7}{2}n^2/[\Lambda(T_{\text{out}})/\Lambda_{23}]$. Since $-1/2 \lesssim \alpha \lesssim 1/2$ for the relevant temperatures, the outer slope of the eigenfunction is expected to lie in the small range $1/3 \lesssim n \lesssim 2/5$ (cf. Fig. 2). The run of the eigenvalue as a function of T_{out} (Fig. 1) reflects the proportionality to $1/\Lambda(T_{\text{out}})$, modulated by n^2 , which accounts for the dependence on the local slope of the cooling function α .

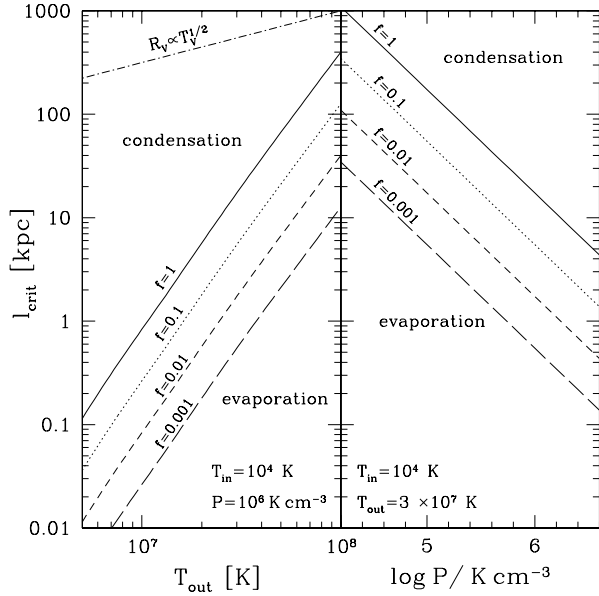


Figure 3. Left: Critical length of a radiatively stabilized filament as a function of the temperature of the ambient medium, at fixed pressure $P = 10^6 \text{ K cm}^{-3}$, for a few values of the suppression factor f . The dot-dashed line represents the self-similar relation between virial temperature and virial radius. Right: Critical length as a function of pressure, at fixed temperature $T = 3 \times 10^7 \text{ K}$, for the same set of values of f as in left panel.

3 APPLICATIONS

3.1 Critical length for filaments

We now discuss the physical implications of the results presented in the previous section. Equation (6) relates the numerical value of λ to the dimensional quantities associated with a filament and its surroundings. If, as explained above, we identify R_{out} with the length of a filament, then this equation yields for a given environment the critical length l_{crit} of filaments, such that smaller filaments evaporate while larger ones grow. Numerically we have

$$l_{\text{crit}} \equiv R_{\text{out}} \simeq 1.4 f^{1/2} \lambda^{1/2} \left(\frac{T_{\text{out}}}{10^7 \text{ K}} \right)^{11/4} \left(\frac{P}{10^6 \text{ K cm}^{-3}} \right)^{-1} \text{ kpc.} \quad (7)$$

This equation indicates that l_{crit} has a strong dependence on the outer temperature ($l_{\text{crit}} \propto T_{\text{out}}^{11/4}$, neglecting the weak dependence of λ on T_{out} ; see Fig. 1), and also is inversely proportional to the pressure P . Even though the dependence of l_{crit} on the thermal conduction suppression factor f is not very strong ($l_{\text{crit}} \propto f^{1/2}$), f can significantly affect l_{crit} because the value of f is very uncertain: $f \sim 1$ seems to be excluded, but different authors give values differing by two orders of magnitude, from a few 10^{-1} to $\sim 10^{-3}$ – see Narayan & Medvedev (2001) for a discussion. We consider values in the range $10^{-3} \lesssim f \lesssim 1$ and discuss the possibility of constraining f from observations of filaments in Section 3.4.

Consider the implications of the dependence of l_{crit} on T_{out} at fixed pressure. The left panel of Fig. 3

shows $l_{\text{crit}}(T_{\text{out}})$ from equation (7), for pressure $P = 10^6 \text{ K cm}^{-3}$, which is a typical value in the core of a cooling-flow galaxy cluster [e.g., for the Perseus cluster, Conselice et al. (2001), Schmidt, Fabian & Sanders (2002); see also Heckman et al. (1989)]. A few values of the suppression factor ($f = 1, 0.1, 0.01, 0.001$) are considered. For given f , the relation $l_{\text{crit}}(T_{\text{out}})$ divides the the diagram in two regions: filaments longer than l_{crit} are condensing, while smaller ones are evaporating. It is apparent from the steep slope of the curves in the diagram that the process of evaporation or condensation of filaments is very sensitive to the temperature of the ambient medium. For a plausible value of the suppression factor, $f \sim 0.01$, at fixed pressure $\sim 10^6 \text{ K cm}^{-3}$, any filament longer than $\sim 0.1 \text{ kpc}$ is condensing in a cluster with ambient temperature $T_{\text{out}} = 10^7 \text{ K}$, while filaments as long as $\sim 10 \text{ kpc}$ are evaporating if $T_{\text{out}} = 6 \times 10^7 \text{ K}$.

Although l_{crit} depends on pressure more weakly than on temperature, pressure also plays an important role in determining the fate of filaments. This is apparent in the right diagram of Fig. 3, where we fix $T_{\text{out}} = 3 \times 10^7 \text{ K}$ and plot l_{crit} as a function of P , for the set of values of f considered above. The diagram shows that, at fixed temperature, in low-pressure clusters virtually all filaments are evaporating (e.g., $l_{\text{crit}} \sim 100 \text{ kpc}$ for $P \sim \text{few} \times 10^4 \text{ K cm}^{-3}$ and $f = 0.01$), but condensation is effective in the highest-pressure ambient gas ($l_{\text{crit}} \sim 1 \text{ kpc}$ for $P \gtrsim 10^6 \text{ K cm}^{-3}$ and $f = 0.01$).

3.2 Time-scales

What are the characteristic time-scales for evaporation and condensation of filaments? A detailed answer to this question would require the solution of the full hydrodynamic equations for non-vanishing mass flow. However, for the purpose of our investigation we are interested in an order of magnitude estimate, which can be obtained by considering that the time variation of temperature is described by a differential equation of the form

$$\frac{dT}{dt} = \frac{T}{t_{\kappa}} - \frac{T}{t_{\text{cool}}}, \quad (8)$$

where t_{κ} and t_{cool} are the thermal conduction and cooling time-scales, respectively. The relation between these time-scales is given by

$$\frac{t_{\kappa}}{t_{\text{cool}}} = \frac{n_e \Lambda(T)}{|\nabla \cdot \mathbf{q}|} \sim \frac{n_e^2 \Lambda(T) l^2}{\kappa(T) T}, \quad (9)$$

because $|\nabla \cdot \mathbf{q}| \sim \kappa(T) T / l^2$, where l is the temperature variation length scale (Begelman & McKee 1990). In the considered case, l is the radial extension of the interface, which is of the order of the filament length (see Section 2). Considering that the equilibrium solution ($l = l_{\text{crit}}$) corresponds to $t_{\kappa} \sim t_{\text{cool}}$, from equation (9) we get

$$t_{\kappa} \sim \left(\frac{l}{l_{\text{crit}}} \right)^2 t_{\text{cool}}, \quad (10)$$

and equation (8) can be approximated as

$$\frac{dT}{dt} = \frac{T}{t_{\text{cool}}} \left[\left(\frac{l_{\text{crit}}}{l} \right)^2 - 1 \right]. \quad (11)$$

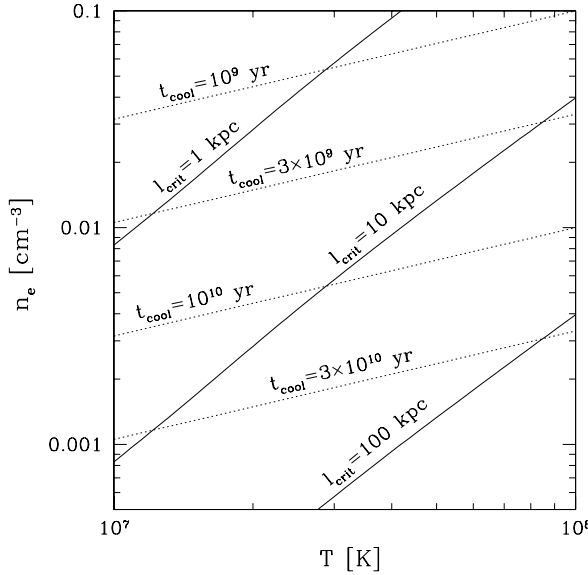


Figure 4. Dotted curves: density–temperature relation for plasma with fixed cooling time ($t_{\text{cool}} = 0.1, 0.3, 1, 3$ in units of 10^{10} yr). Solid curves: density as function of temperature for $l_{\text{crit}} = 1, 10, 100$ kpc and $f = 0.01$ (equation 7).

Consequently, filaments shorter than $\sim \frac{1}{2}l_{\text{crit}}$ evaporate in a fraction $(l/l_{\text{crit}})^2$ of the cooling time, which for example is $\lesssim 300$ Myr within ~ 4 kpc of the centre of the Hydra cluster, (David et al. 2000). Filaments smaller than l_{crit} by a factor $\gtrsim 8$ have evaporation times $\lesssim 5$ Myr that are smaller than their likely dynamical times, l/v , where $v \sim 100 \text{ km s}^{-1}$ is the typical gas velocity estimated from line widths (Sabra et al. 2000 and references therein). On the other hand, equation (11) in the limit $l \gg l_{\text{crit}}$ indicates that, as expected, very long filaments condense on time-scales of the order of the cooling time of the ambient medium.

These considerations strongly support the hypothesis that *only filaments with lengths comparable to the critical length or longer are likely to survive for long enough to be observed*.

3.3 The fate of filaments in cooling-flow and non-cooling-flow clusters

The results presented above have interesting implications, when compared with the properties of observed galaxy clusters.

(i) A first simplistic implication is that, due to the strong dependence of l_{crit} on temperature, in massive (high-temperature) clusters most cold gas structures are evaporating, while even relatively small clouds can survive (and condense) in small (low-temperature) clusters. On the other hand one needs to bear in mind that clusters with higher temperatures have larger virial radii R_V , and it is natural to expect the typical size of clouds to increase proportional to R_V . The left panel of Fig. 3 shows the relation between R_V and the virial temperature ($R_V \propto T_V^{1/2}$) predicted for galaxy clusters un-

der the assumption of self-similarity (the slope of this scaling relation is consistent with that derived from X-ray observations of galaxy clusters; see, e.g., Ettori, De Grandi & Molendi 2002, and references therein). Thus, as is apparent from the diagram, the relation $l_{\text{crit}}(T_{\text{out}})$ is much steeper than the relation between cluster size and temperature. Hence, in the highest-temperature clusters any cold filament is evaporating, while in the lowest-temperature clusters, any resolvable filament is condensing.

(ii) The scenario presented in the previous point would hold under the assumption that the physical properties (gas density and pressure) of clusters of given temperature would not differ significantly from cluster to cluster. In fact, we know this is not the case: for fixed gas temperature, non-cooling-flow clusters (i.e., ones with long cooling times) have, by definition, lower central density (and pressure) than cooling-flow clusters. Thus, as shown by the right panel of Fig. 3, since $l_{\text{crit}} \propto 1/P$, a filament long enough to be condensing in the core of a cooling-flow cluster with central temperature T might evaporate if it were at the centre of a non-cooling-flow cluster with the same temperature (but lower density). This argument suggests that filaments of cold gas are not observed in non-cooling-flow clusters because in these clusters they are evaporated very efficiently, even at the cluster centre. On the other hand, whatever their formation mechanism, filaments are more likely to survive and grow in the denser, higher pressure cores of cooling-flow clusters.

(iii) In a given cooling-flow cluster, T increases as one moves away from the centre, while P falls. Consequently, equation (7) predicts that l_{crit} increases rapidly with distance from the cluster centre. This result explains why, even in the infall or merging scenario for the formation of the filaments, these are observed only in the cooling cores of clusters, and not in the outer regions. For example, in the Perseus cluster, the gas temperature at a distance ~ 100 kpc from the center is roughly twice the central temperature. Also, in the same radial range the pressure decreases by a factor of ~ 2.5 (e.g., Schimdt et al. 2002; Churazov et al. 2003). Thus, equation (7) predicts that l_{crit} grows by over a factor of 10 between the centre and 100 kpc. Interestingly, even in the core, observations indicate that the mean H α emission is a strongly decreasing function of the cluster radius (e.g., Conselice et al. 2001). This result may arise because as one moves out, H α emission from smaller filaments contributes less and less to the overall signal.

We can summarize the points above by considering the relation between l_{crit} and the cooling time of ambient gas. For simplicity, we use the approximate isobaric cooling time $t_{\text{cool}} \simeq 10^4 n_e^{-1} T^{1/2} \text{ yr}$ (where n_e is in cm^{-3} and T in K; e.g., Sarazin 1986), considering the temperature range $10^7 - 10^8 \text{ K}$. The dotted curves in Fig. 4 represent the loci of constant cooling time in density-temperature space, while the solid curves show the loci of constant l_{crit} , for suppression factor $f = 0.01$. We see that if the cooling time is long (as in the cores of non-cooling-flow clusters, and in the outer regions of any cluster), l_{crit} is large, so evaporation is very likely. On the other hand, small l_{crit} corresponds to a short cooling time. Hence it

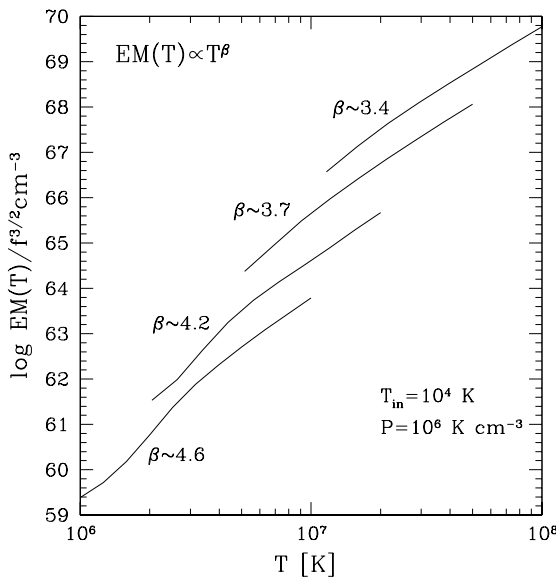


Figure 5. Differential emission measure $EM(T) \equiv n_e^2 dV/d\log T$ as a function of T , corresponding to the critical stationary solution for outer temperatures $T_{\text{out}} = 1, 2, 5, 10$, in units of 10^7 K. f measures the reduction of heat conduction below Spitzer's value. β is the index of the best-fitting power law.

is precisely the physical conditions found in the cores of cooling-flow clusters that favour condensation.

3.4 Suppression of thermal conductivity in the intracluster medium

As outlined in the Introduction, the existence of cold filaments could be used to constrain the value of the thermal conductivity in the ICM. Indeed, we could derive the value of the suppression factor f from equation (7) if we knew all the other quantities involved. Unfortunately, while T_{out} and P are well constrained by observations, it is quite difficult to put strong observational constraints on l_{crit} . A detailed morphological study of the filaments, available only for the Perseus cluster (Conselice et al. 2001), reveals complex structures on different scales. However, we note that even a quite conservative estimate of l_{crit} can lead to interesting constraints on f . For instance, the data suggest that in the Perseus cluster filaments ~ 10 kpc long are present at least up to radii $\sim 40 - 50$ kpc. This means $l_{\text{crit}} \lesssim 10$ kpc, where the ICM temperature and pressure are $\sim 4.5 \times 10^7$ K and $\sim 10^6$ K cm $^{-3}$, respectively (Schmidt et al. 2002). According to equation (7), for these physical properties of the ambient medium, this condition is translated into the *upper limit* $f \lesssim 0.04$ for the thermal conduction suppression factor. This result is compatible with that found by Markevitch et al. (2003) on the basis of observations of cold fronts in A754. We note that a substantially higher efficiency would be required in order for the thermal conductivity to significantly affect cooling flows in the centres of clusters (e.g., Narayan & Medvedev 2001).

In the discussion above we considered the thermal

conduction suppression factor as a global parameter characterizing the ICM in clusters. In fact, the reduction of thermal conductivity could vary from cluster to cluster, or within a given cluster, depending on the detailed properties of the magnetic field. However, there are indications that the effect of the reconnection of the magnetic field lines between the filaments and the ICM would be to enhance the efficiency of heat conduction in the centres of cooling-flow clusters (Soker, Blanton & Sarazin 2004). Thus, at least according to this scenario, it seems reasonable to extend the derived upper limit on f to the ICM in general.

3.5 X-ray emission from conduction fronts of filaments

Here we explore the possibility that the conduction fronts described above can be detected in soft X-rays. This is particularly interesting since Fabian et al. (2003) find soft X-ray emission associated with the brightest H α emission filaments around NGC1275, suggesting that it is produced in the conductive evaporation or condensation of the filaments. We quantify the emission properties of the conduction fronts for the considered cylindrically symmetric clouds, computing the differential emission measure

$$EM(T) \equiv n_e^2 \frac{dV}{d\log T}, \quad (12)$$

where n_e is the electron number density and dV is the volume element. Under the hypothesis of constant pressure $P = n_e T$, the differential emission measure can be related directly to the temperature profile $T(R)$: using $dV = 2\pi l R dR$, with l length of the filament, we get

$$EM(T) = 2\pi l P^2 \frac{R}{T^2} \frac{dR}{d\log T}. \quad (13)$$

As discussed in Section 2, the temperature profile, for given T_{out} , can be considered independent of ξ_{in} at large enough radii ($\xi \gtrsim 10^{-2}$); correspondingly we find that the differential emission measure at $T \gtrsim 0.1 T_{\text{out}}$ is not sensitive to the value of ξ_{in} . Fig. 5 plots the emission measure as a function of T for a subset of values of the outer temperature ($T_{\text{out}} = 1, 2, 5, 10$ in units of 10^7 K). For the normalization of $EM(T)$ we assume $P = 10^6$ K cm $^{-3}$, and $l = l_{\text{crit}} = R_{\text{out}}$, in accordance with the discussion in Section 2. Due to the dependence of l_{crit} on the thermal conduction suppression factor f (equation 7), the normalization of $EM(T)$ is proportional to $f^{3/2}$. Thus it is difficult to make predictions on the absolute value of the emission measure, also because of the strong dependence on pressure. On the other hand, the shape of $EM(T)$ is not affected by these parameters, being determined by the temperature profile, which depends only on the temperature of the ambient medium. As apparent from Fig. 5, in the considered temperature range the differential emission measure can be roughly approximated with a power-law $EM(T) \propto T^\beta$. We find that $EM(T)$ is steeper for lower T_{out} , with best-fitting slope β ranging from $\beta \simeq 3.4$ for $T_{\text{out}} = 10^8$ K to $\beta \simeq 4.6$ for $T_{\text{out}} = 10^7$ K. Accurate measurements of the soft X-ray spectra around

filaments could be interestingly compared with the slopes of these emission measure profiles.

4 CONCLUSIONS

Embedded within cooling flows, one frequently detects filaments of cold gas. Thermal conduction will cause heat to flow into these filaments from the hot ambient gas, with the result that filaments below a critical size will be evaporated. On the other hand radiative cooling is very efficient in cold, dense gas, so larger filaments can survive, and indeed nucleate the cooling of the ambient medium. We have determined the critical filamentary size that divides the two regimes.

The absolute value of this length scale, l_{crit} , is uncertain because we do not know how effectively the magnetic field suppresses thermal conduction. By contrast, the way in which l_{crit} scales with the temperature and pressure of the ambient medium is well determined and leads to suggestive results.

The critical length scale rises sharply with ambient temperature: $l_{\text{crit}} \propto T^{11/4}$, and decreases as P^{-1} with ambient pressure. Consequently, in the Perseus cluster l_{crit} increases by over an order of magnitude between the cluster centre and a radius of 100 kpc, where it is probably larger than 10 kpc. Within a few kiloparsecs of the cluster centre, filaments only a kiloparsec long may either grow, or at least take a long time to evaporate because their lengths are just below the critical value, while such small filaments are rapidly evaporated in the main body of the cluster.

Where do filaments come from in the first place? They cannot emerge spontaneously from the ambient medium because this is thermally stable,² so they must be injected. Simulations of structure formation predict that significant amounts of cold gas fall into clusters (Katz et al. 2003), and the observed filaments could represent just the fraction of this infall that reaches the centre. There is also some indication that extremely close to the cluster centre a small amount of gas cools to filamentary temperatures, and some of this gas could be ejected by the AGN to the radii where filaments are observed.

Whether infall or AGN are responsible for injecting filamentary gas, there is no reason to expect the lengths of the injected filaments to have a characteristic value. It is natural to think in terms of a spectrum of filamentary lengths l , in which the number of filaments decreases with increasing filament length, probably as a power law. Observations of filaments would then be dominated by filaments with $l \sim l_{\text{crit}}$ because shorter filaments would be rapidly evaporated, and larger ones would be rare. The local number density of filaments would be a decreasing

² Balbus (1991) shows that thermal instability is possible in the presence of even a weak magnetic field. However, a weak field can only control low-amplitude perturbations, and buoyant stabilization will reassert itself once the perturbation amplitude is greater than $P_{\text{mag}}/P_{\text{gas}} \sim 10^{-3}$ in clusters. It is also the case that for technical reasons Balbus had to insist on a highly artificial background field for which field-line closure is problematic.

function of l_{crit} , explaining why observed filaments are concentrated near the centres of cooling-flow clusters.

Since filament growth depends on the efficiency of radiative cooling, l_{crit} tends to be small when the cooling time of the ambient medium is short. Hence clusters with short central cooling times, have smaller values of l_{crit} and more filaments than clusters with similar temperatures but longer cooling times. Consequently, it is natural that filaments are only detected in cooling-flow clusters.

For the case of a filament of critical length, we have calculated the temperature profile throughout the interface between gas at $\sim 10^4$ K that emits optical emission lines, and the ambient X-ray emitting plasma. This profile yields the run of differential emission measure with temperature, which can be tested observationally.

As cosmic clustering proceeds, the temperature of gas that is trapped in gravitational potential wells rises as longer and longer length-scale perturbations collapse. This temperature rise causes l_{crit} to rise much faster than the virial radius of the potential well. Hence, while at early times filaments that are much smaller than the system can grow, growth is later restricted to filaments that are comparable in size to the entire system. Consequently, the ability of infalling cold gas to nucleate star formation declines as clustering proceeds.

Semi-analytic models of galaxy formation that can account for the observed slope of the galaxy luminosity function at the faint end need efficient feedback from star formation, and over-produce luminous galaxies (Benson et al. 2003). Binney (2003) has argued that galaxy formation is dominated by infall of cold gas, and that it is the efficient evaporation of filaments in massive systems that suppresses the formation of massive galaxies. Our results make a step towards quantifying this picture.

ACKNOWLEDGMENTS

We thank Luca Ciotti for helpful comments on the manuscript, and the referee, Noam Soker, for interesting suggestions that helped improve the paper. C.N. was partially supported by a grant from Università di Bologna.

REFERENCES

- Balbus, S., 1986, ApJ, 304, 787
- Balbus, S., 1991, ApJ, 372, 25
- Balbus S.A., McKee C.F., 1982, ApJ, 252, 529
- Baum S.A., 1992, PASP, 104, 848
- Begelman M.C., McKee C.F., 1990, ApJ, 358, 375
- Benson A.J., Bower R.G., Frenk C.S., Lacey C.G., Baugh C.M., Cole S., 2003, ApJ, 599, 38
- Binney J., 2003, MNRAS, in press (astro-ph/0308172)
- Binney J., Cowie L.L., 1981, ApJ, 247, 464
- Böhringer H., Fabian A.C., 1989, MNRAS, 237, 1147
- Böhringer H., Hartquist T.W., 1987, MNRAS, 228, 915
- Churazov E., Forman W., Jones C., Böhringer H., 2003, ApJ, 590, 225
- Conselice C.J., Gallagher J.S., Wyse R.F.G., 2001, AJ, 122, 2281
- Cowie L.L., McKee C.F., 1977, ApJ, 211, 135
- Cowie L.L., Songaila A., 1977, Nature, 266, 501

Cowie L.L., Fabian A.C., Nulsen P.E.J., 1980, MNRAS, 191, 399

David L.P., Nulsen P.E.J., McNamara B.R., Forman W., Jones C., Ponman T. Robertson B., Wise M., 2001, ApJ, 557, 546

Donahue M., Voit G.M., 1993, ApJ, 414, L17

Draine B.T., Giuliani J.L., 1984, ApJ, 281, 690

Ettori S., De Grandi S., Molendi S., 2002, A&A, 391, 841

Fabian A.C., 1994, ARA&A, 32, 277

Fabian A.C., Nulsen P.E.J., 1977, MNRAS, 180, 479

Fabian A.C., Sanders J.S., Crawford C.S., Conselice C.J., Gallagher J.S., Wyse R.F.G., 2003, MNRAS, 344, L48

Ferrara A., Shchekinov Yu. 1993, ApJ, 417, 595

Giuliani J.L., 1984, ApJ, 277, 605

Graham R., Langer W.D., 1973, ApJ, 179, 469

Heckman T.M., 1981, ApJ, 250, L59

Heckman T.M., Baum S., van Breugel W.J.M., McCarthy P., 1989, ApJ, 338, 48

Hu E.M., Cowie L.L., Wang Z., 1985, ApJS, 59, 447

Johnstone R.M., Fabian A.C., Nulsen P.E.J., 1987, MNRAS, 224, 75

Katz N., Keres D., Dave R., Weinberg D.H., 2003, in "The IGM/Galaxy Connection: The Distribution of Baryons at $z=0$ ", ASSL Conference Proceedings Vol. 281, J.L. Rosenberg and M.E. Putman eds. (Kluwer Academic Publishers, Dordrecht), 185

Lynds R., 1970, ApJ, 159, L151

Markevitch M. et al. 2000, ApJ, 541, 542

Markevitch M. et al. 2003, ApJ, 586, L19

McKee C.F., Begelman M.C., 1990, ApJ, 358, 392

McKee C.F., Cowie L.L., 1977, ApJ, 215, 213

McNamara B.R., O'Connell R.W., Sarazin C.L., 1996, AJ, 112, 9

Minkowski R., 1957, Canergie Yearbook, 54, 25

Narayan R., Medvedev M.V., 2001, ApJ, 562, L129

Sabra B.M., Shields J.C., Filippenko A.V., 2000, ApJ, 545, 157

Sarazin C.L., 1986, Rev. Mod. Phys., 58, 1

Soker N., Blanton E.L., Sarazin C.L., 2004, in "The Riddle of Cooling Flows in Galaxies and Clusters of Galaxies", Charlottesville, VA, USA. May 31 – June 4, 2003, Eds. Reiprich, T. H., Kempner, J. C., and Soker, N. (astro-ph/0309633)

Soker N., Bregman J.N., Sarazin C.L., 1991, ApJ, 368, 341

Schmidt R.W., Fabian A.C., Sanders J.S., 2002, MNRAS, 337, 71

Sutherland R.S., Dopita M.A., 1993, ApJS, 88, 253

Sparks W.B., 1992, ApJ, 399, 66

Sparks W.B., Macchetto F., Golombek D., 1989, ApJ, 345, 153

Spitzer L., 1962, Physics of Fully Ionized Gases. Wiley-Interscience, New York

Voigt L.M., Fabian A.C., 2003, preprint (astro-ph/0308352)

APPENDIX A: THERMAL CONDUCTION SATURATION PARAMETER

We have hitherto assumed that the thermal conduction is not saturated, so the heat flux is given by the classical equation (2), with the thermal conductivity given by equation (3). The latter formula is derived under the assumption that $l_e/l_T \ll 1$, where l_e is the electron mean free path and $l_T = T/|\nabla T|$ is the temperature scale height. When this condition is violated, equation (2) overestimates the heat flux, which is limited by the thermal speed of electrons, and the modulus of \mathbf{q} is given by the saturated heat flux (Cowie & McKee 1977)

$$q_{\text{sat}} = 0.4 \left(\frac{2k_B T}{\pi m_e} \right)^{1/2} n_e k_B T, \quad (\text{A1})$$

where k_B is the Boltzmann constant, and m_e is the electron mass. Cowie & McKee introduced a discriminant of whether the heat flux in a plasma is saturated: this is the *saturation parameter* $\sigma \equiv q_{\text{cl}}/q_{\text{sat}}$, where $q_{\text{cl}} = \kappa(T)|\nabla T|$ is the modulus of the classical heat flux (equation 2). The critical value that separates the two regimes is $\sigma \sim 1$: for $\sigma \ll 1$ the heat flux is unsaturated, while for $\sigma \gg 1$, equation (A1) applies.

For given T_{out} and corresponding critical temperature profile $T(R)$, the value of the saturation parameter as a function radius in the interface can be obtained combining equations (2), (3), and (A1), and using the relations $n_e = P/T$ and $R_{\text{out}} = l_{\text{crit}}$ (equation 7). Numerically we get

$$\sigma(R) \simeq 8 \times 10^{-3} f^{1/2} \lambda^{-1/2} \left(\frac{T_{\text{out}}}{10^7 \text{ K}} \right)^{1/4} \tau^2 \frac{d\tau}{d\xi}, \quad (\text{A2})$$

where $\xi \equiv R/R_{\text{out}}$, $\tau = \tau(\xi)$ is the normalized temperature profile, and $\lambda = \lambda(T_{\text{out}})$ the corresponding eigenvalue (see Section 2). We note that $\sigma(R)$ is independent of the pressure and scales as the square root of the suppression factor f . Applying equation (A2) to conduction fronts with ambient gas temperature in the considered range $10^6 \lesssim T_{\text{out}} \lesssim 10^8 \text{ K}$, we find in all cases $\sigma(R) \lesssim 10^{-2} f^{1/2}$. Thus, the condition for unsaturated heat conduction ($\sigma \ll 1$) is satisfied throughout the interface, even for the largest values of the suppression factor $f \sim 1$.

This paper has been typeset from a \TeX / \LaTeX file prepared by the author.